NeuroImage 206 (2020) 116189

Contents lists available at ScienceDirect

NeuroImage

journal homepage: www.elsevier.com/locate/neuroimage

Automated anatomical labelling atlas 3

Edmund T. Rolls [a,b,c,*,1], Chu-Chung Huang [a,d,1], Ching-Po Lin [a,d], Jianfeng Feng [a,b,e], Marc Joliot [f]

[a] Institute of Science and Technology for Brain-Inspired Intelligence, Fudan University, Shanghai, 200433, China
[b] Department of Computer Science, University of Warwick, Coventry, CV4 7AL, UK
[c] Oxford Centre for Computational Neuroscience, Oxford, UK
[d] Institute of Neuroscience, National Yang-Ming University, Taipei, Taiwan
[e] School of Mathematical Sciences, School of Life Science and the Collaborative Innovation Center for Brain Science, Fudan University, Shanghai, 200433, PR China
[f] GIN UMR5293, IMN, CNRS, CEA, Université de Bordeaux, Bordeaux, France

ARTICLE INFO

Keywords:
AAL3
Automated anatomical labelling 3
AAL
AAL2
Human brain
Orbitofrontal cortex
Cingulate cortex
Thalamus
Substantia nigra

ABSTRACT

Following a first version AAL of the automated anatomical labeling atlas (Tzourio-Mazoyer et al., 2002), a second version (AAL2) (Rolls et al., 2015) was developed that provided an alternative parcellation of the orbitofrontal cortex following the description provided by Chiavaras, Petrides, and colleagues. We now provide a third version, AAL3, which adds a number of brain areas not previously defined, but of interest in many neuroimaging investigations. The 26 new areas in the third version are subdivision of the anterior cingulate cortex into subgenual, pregenual and supracallosal parts; subdivision of the thalamus into 15 parts; the nucleus accumbens, substantia nigra, ventral tegmental area, red nucleus, locus coeruleus, and raphe nuclei. The new atlas is available as a toolbox for SPM, and can be used with MRIcron.

1. Introduction

The automated anatomical atlas (AAL) (Tzourio-Mazoyer et al., 2002) is widely used in neuroimaging research, including resting state functional magnetic resonance imaging (fMRI). The AAL is available as a toolbox (http://www.gin.cnrs.fr/tools/aal) for SPM (Statistical Parametric Mapping http://www.fil.ion.ucl.ac.uk/spm), with MRIcron (http://www.mccauslandcenter.sc.edu/mricro/mricron), and with the Data Processing Assistant for Resting-State fMRI (DPARSF) (Chao-Gan and Yu-Feng, 2010) (http://rfmri.org/DPARSF). A new regional parcellation of the orbitofrontal cortex was introduced in AAL2 (Rolls et al., 2015) following the description provided by Chiavaras, Petrides, and colleagues (Chiavaras et al., 2001; Chiavaras and Petrides, 2000). Both the original atlas (aal.nii.gz) and the revised atlas AAL2 (aal2.nii.gz) are available at: http://www.gin.cnrs.fr/tools/aal.

We now provide a third version of the automated anatomical atlas, AAL3, which adds a number of brain areas not previously defined, but that are of interest in many neuroimaging investigations including many on reward and memory systems in the brain, and on psychiatric and neurological disorders (Cheng et al., 2018; Conio et al., 2019; Hammerer et al., 2018; Rolls, 2014, 2016; 2018, 2019b; Rolls et al., 2018; Trutti et al., 2019). The new areas in AAL3 are subdivision of the anterior cingulate cortex into subgenual, pregenual and supracallosal parts; the thalamus; the nucleus accumbens, substantia nigra, ventral tegmental area, red nucleus, locus coeruleus and raphe nuclei. The new atlas is available as a toolbox for SPM, AAL3.nii.gz, available at http://www.gin.cnrs.fr/tools/aal-aal3 and https://www.oxcns.org/aal3.html. Descriptions of the new subdivisions appear later in this paper. The AAL atlases are based on a normalized brain in MNI space.

Where we have divided areas from AAL2 into subregions in AAL3, the original area and the new subdivisions cannot appear in the same atlas. We therefore recommend that if users wish to include an area for the anterior cingulate cortex (ACC) that is available in AAL2, but also investigate what applies in its subareas, AAL2 should be run, and then also AAL3 for the subareas. The only areas to which this applies that have been redefined in AAL3 from AAL2 are the anterior cingulate Cortex (ACC) the thalamus, and the Caudate nucleus and Putamen.

Caution is advised in the use of some of the smaller regions defined in

* Corresponding author. University of Warwick, Department of Computer Science. Coventry CV4 7AL, UK..
E-mail address: Edmund.Rolls@oxcns.org (E.T. Rolls).
URL: https://www.oxcns.org (E.T. Rolls).
[1] These authors contributed equally to this work.

https://doi.org/10.1016/j.neuroimage.2019.116189
Received 7 May 2019; Received in revised form 29 August 2019; Accepted 11 September 2019
Available online 12 September 2019

the AAL3. This regions to which this caution applies include the locus coeruleus, the substantia nigra pars compacta, the ventral tegmental area, and the raphe nuclei. This applies because with such small regions, typical registration would not be sufficient for the areas voxels to be identified using AAL3 in most individuals brains. For example, this caution applies to the locus coeruleus region in AAL3, because the locus coeruleus is only one 2x2x2 mm^3 voxel thick in AAL3. That means that identification of the relevant voxels in each individual's brain is needed, using approaches that have been developed for the habenula (Lawson et al., 2013).

2. Description of the new areas in AAL3

Table 1 provides notes on the parcellation of the thalamus adopted in AAL3. Table 2 shows the areas defined in AAL2, with the areas that have changed in AAL3 shown in italics. Table 3 shows the new areas in AAL3, together with the terms used to name each area that will appear in SPM, MRIcron, etc, together with suggested abbreviations. The numbers shown in column 1 of Table 3 are also provided in the output of AAL3. Because in AAL2 the numbers 95–120 are used for the cerebellum, we start the new areas in AAL3 at 121–150 for the thalamus, with the other new areas continuing from 151 as shown in Table 3. The original numbering in AAL2 for the anterior cingulate cortex (35, 36) and thalamus (81, 82) is left empty in AAL3 because finer parcellations of these regions are provided in AAL3. Thus, the total number of parcellations in AAL3 is 166, with the maximum label number 170. Thus most of the numbers used in AAL2 remain the same in AAL3. AAL3 mainly adds new areas starting at number 121.

2.1. Thalamus

The parcellation of the thalamic nuclei adopted was based on that of (Iglesias et al., 2018). In the present work, we firstly reconstructed the high-resolution version of the single-subject T1 image (colin27: the one used in AAL) using the Freesurfer software. The T2-weighted image of colin27 (Aubert-Broche et al., 2006) was used as an additional MRI volume to obtain a more reliable result in the segmentation module (Iglesias et al., 2018). Table 1 shows the AAL3 parcellation for the thalamus, which is also illustrated in Fig. 1. The definition column shows where we have combined divisions of Iglesias et al., in order to combine nuclei, where useful, in order to reduce the number of very small divisions (with e.g. fewer voxels than 10), which would probably not yield reliable MRI data unless special registration for such small groups of voxels was performed. The definition column in Table 1 refers to some of the divisions named by Iglesias et al. The nucleus limitans (or suprageniculate nucleus) is a small nucleus of 12 voxels in the posterior group which was not included in AAL3. The reticular nucleus of the thalamus is a thin shell that surrounds the thalamus, is difficult to parcellate, and so was not included in AAL3.

2.2. Nucleus accumbens

The ventral striatum includes the nucleus accumbens and the olfactory tubercle (Choi et al., 2017). A region OLF which includes the olfactory tubercle is already defined in AAL and AAL2. To help with neuroimaging investigations of the ventral striatum, we have included a new area in AAL3, the nucleus accumbens. Its parcellation in AAL3 was guided by the identification of the nucleus accumbens in the Harvard-Oxford subcortical atlas (Desikan et al., 2006), and especially by (Choi et al., 2017). What was described by (Choi et al., 2017) was used to identify the boundaries of the nucleus accumbens in the single-subject atlas. For those who wish to use a region that could be termed ventral striatum in neuroimaging analyses, we suggest a combination of the nucleus accumbens and OLF in AAL3. Because the nucleus accumbens was included in part of what was defined as caudate and putamen in AAL and AAL2, both the caudate and putamen have decreased a little in AAL3.

Table 1
The parcellation of the thalamic nuclei included in AAL3. The volumes listed are the average of the left and right regions defined in the 1x1x1 mm^3 resolution atlas, aal3_1 mm. The standard 2x2x2 mm^3 resolution atlas is aal3.

Group	AAL3 Abbreviation	Nucleus	Volume (mm^3)	Definition
Anterior	Thal_AV	Anteroventral	154	We include the anterior medial and anterior dorsal nuclei into the AV.
Lateral	Thal_LP	Lateral posterior	198	LP includes the laterodorsal nucleus (LD) which has only 33.5 voxels.
Ventral	Thal_VA	Ventral anterior	610	The Ventral anterior magnocellular (VAmc 13.5 voxels) and Ventromedial (VM less than 10 voxels) have been grouped into VA
	Thal_VL	Ventral lateral	2096	The VL nucleus includes the Ventral lateral anterior (VLa 879 voxels) and the Ventral lateral posterior (VLp 1213 voxels).
	Thal_VPL	Ventral posterolateral	1276.5	The medial portion (ventral posteromedial nucleus) is included in our definition of VPL.
Intralaminar	Thal_IL	Intralaminar	428.5	The Intralaminar nuclei (IL) include Central medial (CeM 64 voxels), Central lateral (CL 18.5 voxels), Paracentral (Pc 4 voxels), Centromedian (CM 297.5 voxels), and the Parafascicular (Pf 6048 voxels) nuclei.
Medial	Thal_RE	Reuniens	8	The reuniens nucleus is a midline thalamic nucleus sometimes termed the medial ventral nucleus (MV-re). The parataenial (Pt) midline thalamic nucleus is so small (7 voxels) that we have not included it.
	Thal_MDm	Mediodorsal medial magnocellular	907	
	Thal_MDl	Mediodorsal lateral parvocellular	278.5	
Posterior	Thal_LGN	Lateral geniculate	234	
	Thal_MGN	Medial Geniculate	174.5	
	Thal_PuA	Pulvinar anterior	211	
	Thal_PuM	Pulvinar medial	1311.5	
	Thal_PuL	Pulvinar lateral	257	
	Thal_PuI	Pulvinar inferior	205	

In AAL3, we ensured that the voxels in the nucleus accumbens and OLF were contiguous.

2.3. Locus coeruleus

The voxels in the locus coeruleus were defined as described by (Betts et al., 2017), and the actual template used was very helpfully provided by

Table 2
The anatomical regions defined in each hemisphere and their label in the automated anatomical labelling atlas AAL2. The regions that have been redefined in AAL3 are shown in italics. Column 4 provides a set of possible abbreviations for the anatomical descriptions.

NO.	ANATOMICAL DESCRIPTION	LABEL aal2.nii.gz	POSSIBLE ABBREVIATION
1,2	Precentral gyrus	Precentral	PreCG
3, 4	Superior frontal gyrus, dorsolateral	Frontal_Sup	SFG
5, 6	Middle frontal gyrus	Frontal_Mid	MFG
7, 8	Inferior frontal gyrus, opercular part	Frontal_Inf_Oper	IFGoperc
9, 10	Inferior frontal gyrus, triangular part	Frontal_Inf_Tri	IFGtriang
11, 12	IFG pars orbitalis,	Frontal_Inf_Orb	IFGorb
13, 14	Rolandic operculum	Rolandic_Oper	ROL
15, 16	Supplementary motor area	Supp_Motor_Area	SMA
17, 18	Olfactory cortex	Olfactory	OLF
19, 20	Superior frontal gyrus, medial	Frontal_Sup_Med	SFGmedial
21, 22	Superior frontal gyrus, medial orbital	Frontal_Med_Orb	PFCventmed
23, 24	Gyrus rectus	Rectus	REC
25, 26	Medial orbital gyrus	OFCmed	OFCmed
27, 28	Anterior orbital gyrus	OFCant	OFCant
29, 30	Posterior orbital gyrus	OFCpost	OFCpost
31, 32	Lateral orbital gyrus	OFClat	OFClat
33, 34	Insula	Insula	INS
35, 36	*Anterior cingulate & paracingulate gyri*	Cingulate_Ant	ACC
37, 38	Middle cingulate & paracingulate gyri	Cingulate_Mid	MCC
39, 40	Posterior cingulate gyrus	Cingulate_Post	PCC
41, 42	Hippocampus	Hippocampus	HIP
43, 44	Parahippocampal gyrus	ParaHippocampal	PHG
45, 46	Amygdala	Amygdala	AMYG
47, 48	Calcarine fissure and surrounding cortex	Calcarine	CAL
49, 50	Cuneus	Cuneus	CUN
51, 52	Lingual gyrus	Lingual	LING
53, 54	Superior occipital gyrus	Occipital_Sup	SOG
55, 56	Middle occipital gyrus	Occipital_Mid	MOG
57, 58	Inferior occipital gyrus	Occipital_Inf	IOG
59, 60	Fusiform gyrus	Fusiform	FFG
61, 62	Postcentral gyrus	Postcentral	PoCG
63, 64	Superior parietal gyrus	Parietal_Sup	SPG
65, 66	Inferior parietal gyrus, excluding supramarginal and angular gyri	Parietal_Inf	IPG
67, 68	SupraMarginal gyrus	SupraMarginal	SMG
69, 70	Angular gyrus	Angular	ANG
71, 72	Precuneus	Precuneus	PCUN
73, 74	Paracentral lobule	Paracentral_Lobule	PCL
75, 76	*Caudate nucleus*	Caudate	CAU
77, 78	*Lenticular nucleus, Putamen*	Putamen	PUT
79, 80	Lenticular nucleus, Pallidum	Pallidum	PAL
81, 82	*Thalamus*	Thalamus	THA
83, 84	Heschl's gyrus	Heschl	HES
85, 86	Superior temporal gyrus	Temporal_Sup	STG
87, 88	Temporal pole: superior temporal gyrus	Temporal_Pole_Sup	TPOsup
89, 90	Middle temporal gyrus	Temporal_Mid	MTG
91, 92	Temporal pole: middle temporal gyrus	Temporal_Pole_Mid	TPOmid
93, 94	Inferior temporal gyrus	Temporal_Inf	ITG
95, 96	Crus I of cerebellar hemisphere	Cerebellum_Crus1	CERCRU1
97, 98	Crus II of cerebellar hemisphere	Cerebellum_Crus2	CERCRU2
99, 100	Lobule III of cerebellar hemisphere	Cerebellum_3	CER3
101, 102	Lobule IV, V of cerebellar hemisphere	Cerebellum_4_5	CER4_5
103, 104	Lobule VI of cerebellar hemisphere	Cerebellum_6	CER6
105, 106	Lobule VIIB of cerebellar hemisphere	Cerebellum_7b	CER7b
107, 108	Lobule VIII of cerebellar hemisphere	Cerebellum_8	CER8
109, 110	Lobule IX of cerebellar hemisphere	Cerebellum_9	CER9
111, 112	Lobule X of cerebellar hemisphere	Cerebellum_10	CER10
113	Lobule I, II of vermis	Vermis_1_2	VER1_2
114	Lobule III of vermis	Vermis_3	VER3
115	Lobule IV, V of vermis	Vermis_4_5	VER4_5
116	Lobule VI of vermis	Vermis_6	VER6
117	Lobule VII of vermis	Vermis_7	VER7
118	Lobule VIII of vermis	Vermis_8	VER8
119	Lobule IX of vermis	Vermis_9	VER9
120	Lobule X of vermis	Vermis_10	VER10

Table 3
The extra anatomical regions defined AAL3 in each hemisphere and their label. Column 4 provides a set of possible abbreviations for the anatomical descriptions. In AAL3, the label shown in column 3 is followed by the number shown in column 1. In most cases, the first number in a row is for the left hemisphere, and the second number is for the right hemisphere. This does not apply to the raphe nuclei, which are midline structures.

NO.	ANATOMICAL DESCRIPTION	LABEL AAL3.nii.gz	POSSIBLE ABBREVIATION
121, 122	Thalamus, Anteroventral Nucleus	Thal_AV	tAV
123, 124	Lateral posterior	Thal_LP	tLP
125, 126	Ventral anterior	Thal_VA	tVA
127, 128	Ventral lateral	Thal_VL	tVL
129, 130	Ventral posterolateral	Thal_VPL	tVPL
131, 132	Intralaminar	Thal_IL	tIL
133, 134	Reuniens	Thal_Re	tRe
135, 136	Mediodorsal medial magnocellular	Thal_MDm	tMDm
137, 138	Mediodorsal lateral parvocellular	Thal_MDl	tMDl
139, 140	Lateral geniculate	Thal_LGN	tLGN
141, 142	Medial Geniculate	Thal_MGN	tMGN
143, 144	Pulvinar anterior	Thal_PuA	tPuA
145, 146	Pulvinar medial	Thal_PuM	tPuM
147, 148	Pulvinar lateral	Thal_PuL	tPuL
149, 150	Pulvinar inferior	Thal_PuI	tPuI
151, 152	Anterior cingulate cortex, subgenual	ACC_sub	ACCsub
153, 154	Anterior cingulate cortex, pregenual	ACC_pre	ACCpre
155, 156	Anterior cingulate cortex, supracallosal	ACC_sup	ACCsup
157, 158	Nucleus accumbens	N_Acc	Nacc
159, 160	Ventral tegmental area	VTA	VTA
161, 162	Substantia nigra, pars compacta	SN_pc	SNpc
163, 164	Substantia nigra, pars reticulata	SN_pr	SNpr
165, 166	Red nucleus	Red_N	RedN
167, 168	Locus coeruleus	LC	LC
169	Raphe nucleus, dorsal	Raphe_D	RapheD
170	Raphe nucleus, median	Raphe_M	RapheM

these authors. The locus coeruleus mask was defined in a high-resolution (0.5 mm^3) MNI152 template. To obtain accurate transformation between different MNI template, LC mask was nonlinearly registered into colin27 single-subject T1 template using the white matter segments as references. Caution is advised in use of the locus coeruleus region in AAL3 without checking the exact voxels in each individual, because the locus coeruleus is only one 2x2x2 mm^3 voxel thick in AAL3.

2.4. Anterior cingulate cortex

The ACC of AAL and AAL2 is a large region that includes the subgenual cingulate cortex area 25, and also pregenual and supracallosal components that appear to have different functions (Grabenhorst and

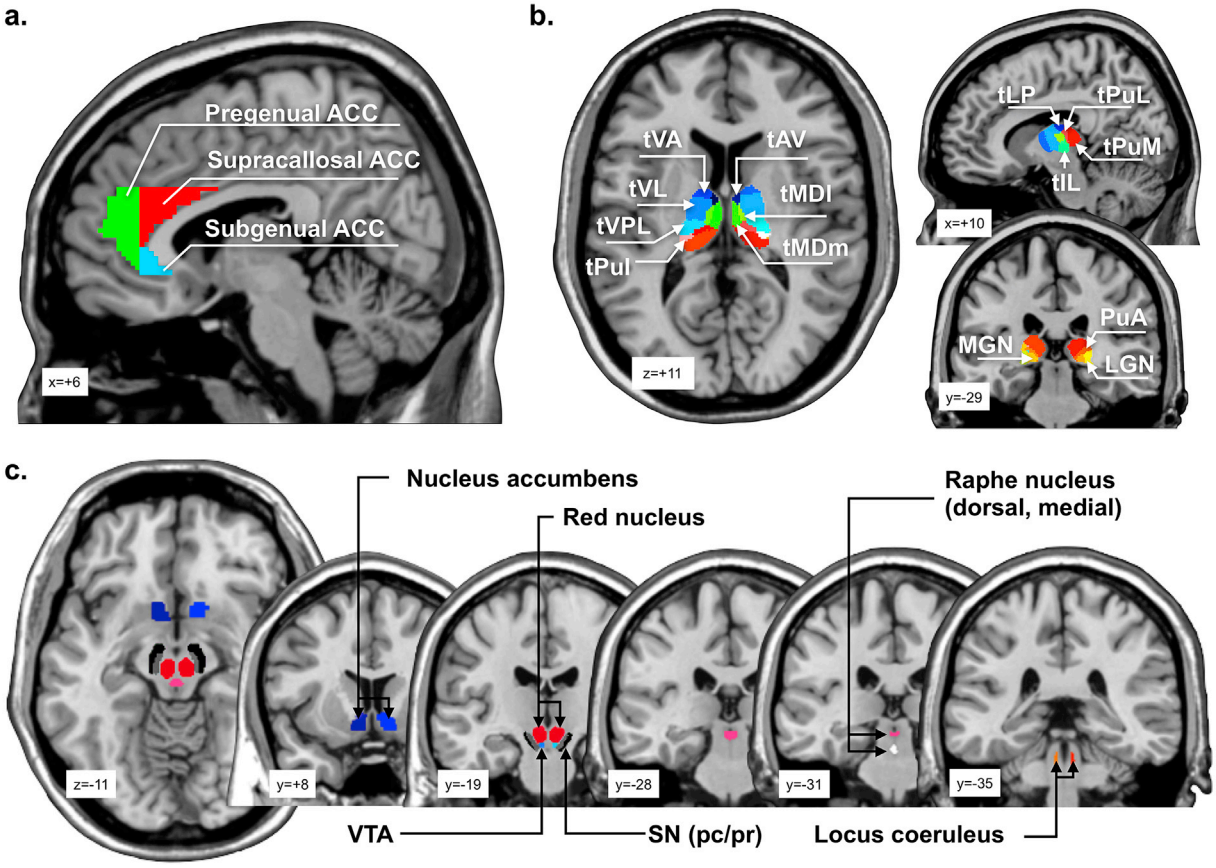

Fig. 1. Illustration of the newly added parcellations in AAL3. The new regions include (a) subgenual, pregenual, and supracallosal divisions of the anterior cingulate cortex (ACC), (b) the thalamic nuclei (for abbreviations see Table 1), and (c) the nucleus accumbens, ventral tegmental area (VTA), red nucleus, substantia nigra (pars compacta and pars reticulata), raphe nuclei (dorsal and medial), and the locus coeruleus.

Rolls, 2011; Rolls, 2014, 2019b, c). Further, recent parcellation studies based on the connectivity of each voxel with other AAL2 areas provide evidence for different functional connectivity of the pregenual and supracallosal anterior cingulate cortex (Du et al., 2019; Rolls et al., 2018, 2019). In AAL3 we have accordingly divided ACC into three parts. For simplicity, these parts were identified by a vertical plane at the anterior border of the genu of the corpus callosum (at Y = 37), and by a horizontal plane through the genu of the corpus callosum at the level of its most anterior part (at Z = 3). The subgenual part was defined as the part of the ACC below and posterior to these two planes. The pregenual part was specified as the part anterior to the vertical plane. The supracallosal part was identified as that posterior to the vertical plane and above the horizontal plane. (In detail, pregenual was defined as Y≥37, subgenual as Y ≤ 36 and Z ≤ 2), and/supra-callosal as Y≥37 and Z ≥ 3, in the MNI coordinates used. We note that the supracallosal part of ACC (ACCsup) may extend posteriorly into what is considered part of the mid-cingulate cortex as defined by Vogt (Rolls, 2019a, b; Vogt, 2016, 2019).

2.5. Substantia nigra, ventral tegmental area, and red nucleus

None of these are defined in AAL or AAL2. In AAL3, these three regions are included, using a template from (Pauli et al., 2018). Separate parts of the substantia nigra in AAL3 are the pars reticulata and pars compacta. Again, we caution use of the substantia nigra pars compacta parcel in AAL3 without checking the exact voxels in each individual, because the pars compacta is thin.

2.6. Raphe nuclei

The voxels in the raphe nuclei were defined as described by (Beliveau et al., 2015), and with separate divisions for the dorsal and median raphe nuclei. The actual template used was very helpfully provided by these authors. The original raphe masks were defined in the ICBM152 standard space. In the present work, we nonlinearly registered the masks into the colin27 single-subject template using the white matter segment of each template as the source and reference. We caution use of the raphe nuclei in AAL3 without checking the exact voxels in each individual, because the raphe nuclei are small and thin. Care must be taken in each participant to ensure that voxels do not overlap with the cerebral aqueduct or the 4th ventricle.

Data and code availability

All data and code for the automated anatomical labelling atlas 3 is available in the SPM toolbox made available in association with this paper at the authors' websites including http://www.gin.cnrs.fr/en/tools and https://www.oxcns.org/aal3.html.

Acknowledgements

The voxels in the locus coeruleus were defined as described by (Betts et al., 2017), and the actual template used was very helpfully provided by these authors. The voxels in the raphe nuclei were defined as described by (Beliveau et al., 2015), and the actual template used was very helpfully provided by these authors. The authors thank Dr Nathalie Tzourio-Mazoyer (GIN UMR5293, CNRS CEA Université de Bordeaux, Bordeaux, France), an author of previous versions of the automated anatomical labelling atlas, for her help and advice with this version. J Feng is partially supported by the key project of Shanghai Science and Technology Innovation Plan (No. 15JC1400101 and No. 16JC1420402),

Shanghai Municipal Science and Technology Major Project (No.2018SHZDZX01) and ZJLab, and the National Natural Science Foundation of China (Grant No. 71661167002 and No. 91630314). Support for this work was also provided by the Key Laboratory of Computational Neuroscience and Brain- Inspired Intelligence (Fudan University), Ministry of Education, China (NO. B18015).

References

Aubert-Broche, B., Evans, A.C., Collins, L., 2006. A new improved version of the realistic digital brain phantom. Neuroimage 32, 138–145.

Beliveau, V., Svarer, C., Frokjaer, V.G., Knudsen, G.M., Greve, D.N., Fisher, P.M., 2015. Functional connectivity of the dorsal and median raphe nuclei at rest. Neuroimage 116, 187–195.

Betts, M.J., Cardenas-Blanco, A., Kanowski, M., Jessen, F., Duzel, E., 2017. In vivo MRI assessment of the human locus coeruleus along its rostrocaudal extent in young and older adults. Neuroimage 163, 150–159.

Chao-Gan, Y., Yu-Feng, Z., 2010. DPARSF: a MATLAB toolbox for "pipeline" data analysis of resting-state fMRI. Front. Syst. Neurosci. 4, 13.

Cheng, W., Rolls, E.T., Qiu, J., Xie, X., Wei, D., Huang, C.C., Yang, A.C., Tsai, S.J., Li, Q., Meng, J., Lin, C.P., Xie, P., Feng, J., 2018. Increased functional connectivity of the posterior cingulate cortex with the lateral orbitofrontal cortex in depression. Transl. Psychiatry 8, 90.

Chiavaras, M.M., LeGoualher, G., Evans, A., Petrides, M., 2001. Three-dimensional probabilistic atlas of the human orbitofrontal sulci in standardized stereotaxic space. Neuroimage 13, 479–496.

Chiavaras, M.M., Petrides, M., 2000. Orbitofrontal sulci of the human and macaque monkey. J. Comp. Neurol. 422, 35–54.

Choi, E.Y., Ding, S.L., Haber, S.N., 2017. Combinatorial inputs to the ventral striatum from the temporal cortex, frontal cortex, and amygdala: implications for segmenting the striatum. eNeuro 4.

Conio, B., Martino, M., Magioncalda, P., Escelsior, A., Inglese, M., Amore, M., Northoff, G., 2019. Opposite effects of dopamine and serotonin on resting-state networks: review and implications for psychiatric disorders. Mol. Psychiatry. https://doi.org/10.1038/s41380-019-0406-4.

Desikan, R.S., Segonne, F., Fischl, B., Quinn, B.T., Dickerson, B.C., Blacker, D., Buckner, R.L., Dale, A.M., Maguire, R.P., Hyman, B.T., Albert, M.S., Killiany, R.J., 2006. An automated labeling system for subdividing the human cerebral cortex on MRI scans into gyral based regions of interest. Neuroimage 31, 968–980.

Du, J., Rolls, E.T., Cheng, W., Li, Y., Gong, W., Qiu, J., Feng, J., 2019. Functional connectivity of the orbitofrontal cortex, anterior cingulate cortex, and inferior frontal gyrus in humans. Cortex (in revision).

Grabenhorst, F., Rolls, E.T., 2011. Value, pleasure, and choice in the ventral prefrontal cortex. Trends Cogn. Sci. 15, 56–67.

Hammerer, D., Callaghan, M.F., Hopkins, A., Kosciessa, J., Betts, M., Cardenas-Blanco, A., Kanowski, M., Weiskopf, N., Dayan, P., Dolan, R.J., Duzel, E., 2018. Locus coeruleus integrity in old age is selectively related to memories linked with salient negative events. Proc. Natl. Acad. Sci. U.S.A. 115, 2228–2233.

Iglesias, J.E., Insausti, R., Lerma-Usabiaga, G., Bocchetta, M., Van Leemput, K., Greve, D.N., van der Kouwe, A., Alzheimer's Disease Neuroimaging, I., Fischl, B., Caballero-Gaudes, C., Paz-Alonso, P.M., 2018. A probabilistic atlas of the human thalamic nuclei combining ex vivo MRI and histology. Neuroimage 183, 314–326.

Lawson, R.P., Drevets, W.C., Roiser, J.P., 2013. Defining the habenula in human neuroimaging studies. Neuroimage 64, 722–727.

Pauli, W.M., Nili, A.N., Tyszka, J.M., 2018. A high-resolution probabilistic in vivo atlas of human subcortical brain nuclei. Sci Data 5, 180063.

Rolls, E.T., 2014. Emotion and Decision-Making Explained. Oxford University Press, Oxford.

Rolls, E.T., 2016. Cerebral Cortex: Principles of Operation. Oxford University Press, Oxford.

Rolls, E.T., 2018. The Brain, Emotion, and Depression. Oxford University Press, Oxford.

Rolls, E.T., 2019a. The cingulate cortex and limbic systems for action, emotion, and memory. In: Vogt, B.A. (Ed.), Handbook of Clinical Neurology: Cingulate Cortex. Elsevier, New York.

Rolls, E.T., 2019b. The cingulate cortex and limbic systems for emotion, action, and memory. Brain Struct. Funct. https://doi.org/10.1007/s00429-00019-01945-00422.

Rolls, E.T., 2019c. The Orbitofrontal Cortex. Oxford University Press, Oxford.

Rolls, E.T., Cheng, W., Du, J., Wei, D., Qiu, J., Dai, D., Zhou, Q., Xie, P., Feng, J., 2019. Functional Connectivity of the Right Inferior Frontal Gyrus and Orbitofrontal Cortex in Depression (submitted for publication).

Rolls, E.T., Cheng, W., Gong, W., Qiu, J., Zhou, C., Zhang, J., Lv, W., Ruan, H., Wei, D., Cheng, K., Meng, J., Xie, P., Feng, J., 2018. Functional connectivity of the anterior cingulate cortex in depression and in health. Cerebr. Cortex. https://doi.org/10.1093/cercor/bhy1236.

Rolls, E.T., Joliot, M., Tzourio-Mazoyer, N., 2015. Implementation of a new parcellation of the orbitofrontal cortex in the automated anatomical labeling atlas. Neuroimage 122, 1–5.

Trutti, A.C., Mulder, M.J., Hommel, B., Forstmann, B.U., 2019. Functional neuroanatomical review of the ventral tegmental area. Neuroimage 191, 258–268.

Tzourio-Mazoyer, N., Landeau, B., Papathanassiou, D., Crivello, F., Etard, O., Delcroix, N., Mazoyer, B., Joliot, M., 2002. Automated anatomical labeling of activations in SPM using a macroscopic anatomical parcellation of the MNI MRI single-subject brain. Neuroimage 15, 273–289.

Vogt, B.A., 2016. Midcingulate cortex: structure, connections, homologies, functions and diseases. J. Chem. Neuroanat. 74, 28–46.

Vogt, B.A. (Ed.), 2019. Handbook of Clinical Neurology: Cingulate Cortex, 3 ed. Elsevier, New York.